# Nonlinear dynamics of self-organized microstructure under irradiation

D. Walgraef* and N. M. Ghoniem
*Mechanical, Aerospace and Nuclear Engineering Department, The University of California at Los Angeles, Los Angeles, California 90024*
(Received 11 October 1994)

We analyze the formation and evolution of point and line defect microstructure in irradiated materials. The effects of irradiation on materials are described by dynamical conservation equations for two mobile atomic size species (vacancies and interstitial atoms), and two basic immobile elements of the microstructure (vacancy and interstitial clusters). It is shown that, under specific irradiation and material conditions, uniform vacancy and interstitial cluster populations become unstable, forming large-scale spatially organized distributions. The structure and symmetry of these organized distributions are shown to evolve with time. The selection and stability of the resulting microstructure are studied in the quasistatic approximation and in the weakly nonlinear regime around the bifurcation point. It is shown that point defect recombination does not affect the long time evolution of the microstructure, and that the final pattern should correspond to planar wall structures, in agreement with experimental observations. Time-dependent evolution of self-organized microstructure is demonstrated for various irradiation and temperature conditions, placing special emphasis on the role of dislocation bias and direct cascade clustering on the self-organization of extended defects.

## I. INTRODUCTION

Many irradiated materials present several types of microstructure which correspond to the spatial organization of defect populations. Well-known examples are void[1–3] and bubble lattices,[4–6] precipitate ordering,[7] defect walls, and vacancy loop ordering.[8–10] In particular, the spatial ordering of vacancy dislocation loops occurs frequently in metals and alloys irradiated at moderate doses and high temperatures.[11] The uniform distribution of loops created by the collapse of cascades becomes unstable beyond some threshold, which is determined by various material and irradiation parameters (e.g., the irradiation dose, damage rate, bias in the migration of point defects to loops and network dislocations, and temperature). In a preceeding study,[12] we analyzed this phenomenon in the framework of a dynamical model which considers the two major elements of irradiated microstructures, namely, vacancy and interstitial clusters. In this regard, we model the effects of irradiation on materials in the form of dynamical equations for two mobile atomic size species (vacancies and interstitial atoms), and two basic immobile elements of the microstructure (vacancy and interstitial clusters). These equations are based on the fundamental elements of defect dynamics, namely, point defect creation, recombination, and migration to the microstructure. In the sink-dominated regime, we computed the instability threshold for vacancy cluster ordering in a quasistatic approximation since one has to take into account the continuous evolution of the structure. We also performed a weakly nonlinear analysis showing that, as irradiation proceeds, one should expect a transition from a uniform distribution of loops to bcc and finally to planar wall structures.

Recent molecular dynamics computer simulations of collision cascades have shown that interstitial clusters can be directly produced in the neighborhood of cascades.[13] Implications of this direct production process to swelling and other macroscopic phenomena are discussed by Singh and co-workers.[14,15] The aim of the present work is to expand on earlier analysis, with the following new aspects: (1) incorporation of direct interstitial loop production in the dynamical model, (2) explicit account of point defect recombination in stability analysis, and (3) presentation of a general framework for nonlinear stability of slowly evolving microstructure.

It is experimentally established that the formation of organized microstructure under irradiation requires the production of defects in cascades. Thus, experimental observations of organized microstructure have only been made on either neutron or ion irradiation. To date, no observation of ordered microstructure were reported for materials irradiated with electrons. An example of void lattice formation under neutron irradiation is shown in Fig. 1, where the alloy titanium-zirconium-molybdenum (TZM) is irradiated at 450 °C with fast neutrons. The neutron fluence is $3.5\times10^{2}6$ n/m$^2$, and the magnification shown is 200 000. The emerging void lattice is isomorphic with the bcc lattice structure of TZM.

Jaeger, Ehrhart, and Schilling conducted 3 MeV proton irradiation of Ni and Cu, up to 2 dpa. They observed a large concentration of stacking fault tetrahedrons (SFT's) of average diameters less than 5.5 nm. At the lowest dose levels ($\simeq$0.01 dpa), the distribution of SFT's is quite homogeneous. At doses of $\simeq$0.1 dpa, fluctuations of point defect clusters were observed, and regions of locally dense clusters along {001} matrix directions start to appear. As the dose is increased to $\simeq$0.65 dpa, the periodicity of defect clusters becomes more pronounced, although strong local variations were still observable. Figure 2 shows the formation of well-developed periodic walls of defect clusters in Cu at a dose of 2 dpa.

0163-1829/95/52(6)/3951(12)/$06.00  

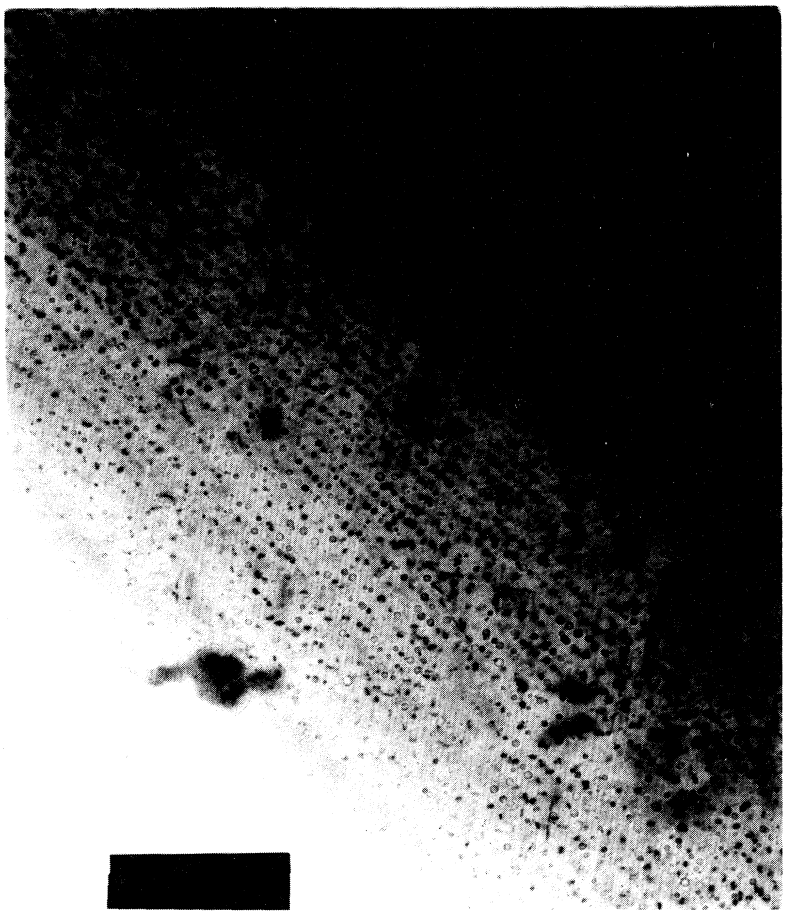

FIG. 1. Void lattice in the alloy TZM, irradiated at 450 °C. The fast neutron flux ($E > 0.1$ MeV) is $3.5 \times 10^26$ n/m$^2$, and the magnification is 200 000 (courtesy of J. Evans).

The specimens were imaged in a {110} projection [Fig. 2(a)], and in a {100} projection [Fig. 2(b)]. The observed wavelength of these wall arrangements is about 60 nm. The walls are reported to contain a high density of dislocation loops and SFT's.

These experimental observations indicate that the immediate condensation of vacancies during the collisional phase of cascades, in the form of small vacancy clusters (e.g., loops of SFT's), is a prerequisite for the emergence of an organized microstructure. In the model presented here, the microstructure is divided into two components, an interstitial dislocation loop component and a vacancy

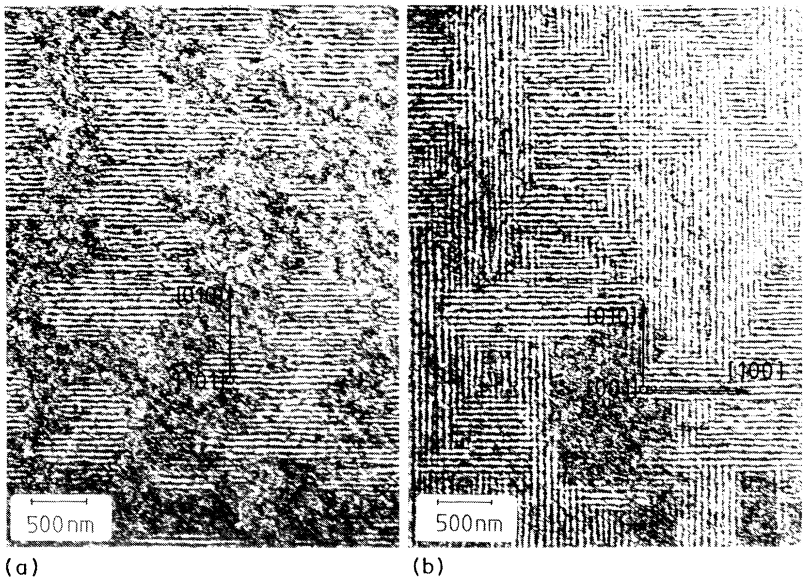


FIG. 2. Formation of planar periodic defect walls in proton-irradiated copper at a dose of 2 dpa. Imaging is in the {110} projection in (a) and in the {100} projection in (b) (courtesy of W. Jaeger).

cluster component. Vacancy clusters are assumed to form directly from cascades at an initial radius $r_V^0$, and may *shrink* forming a small loop or SFT. The model can be extended to treat the case of *growing* vacancy clusters to form a void lattice, but this will not be attempted here.

In Sec. II of this paper, we accordingly reformulate the kinetic equations describing defect dynamics under irradiation. In Sec. III we derive the evolution equations for the loops. In Sec. IV we perform the linear stability analysis of uniform loop distributions and derive the conditions for instability. We then proceed to the weakly nonlinear analysis around the instability threshold in Sec. V and present the conclusions in Sec. VI. Mathematical details are discussed in the appendixes.

## II. THE RATE THEORY MODEL OF MICROSTRUCTURE EVOLUTION

In order to explicitly account for the effect of direct interstitial loop production on the evolution of defect populations, we propose a rate theory dynamical model. Radiation-produced defects are represented by two equations for point defects, which are considered as mobile species, and a set of equations describing the evolution of loops, which are considered as immobile species. Since point defects are the only mobile components of the microstructure, their rate equations would include spatial operators. Immobile microstructures are represented by interstitial and vacancy clusters as shown below:

$$
\begin{aligned}
\partial_t c_i &= K(1-\epsilon_i) - \alpha c_i c_v + D_i \nabla^2 c_i \\
&\quad - D_i c_i (Z_{iN}\rho_N + Z_{iV}\rho_V + Z_{iI}\rho_I) , \\
\partial_t c_v &= K(1-\epsilon_v) - \alpha c_i c_v + D_v \nabla^2 c_v \\
&\quad - D_v [Z_{vN}(c_v - \bar{c}_{vN})\rho_N \\
&\qquad + Z_{vV}(c_v - \bar{c}_{vV})\rho_V \\
&\qquad + Z_{vI}(c_v - \bar{c}_{vI})\rho_I] , \\
\partial_t \rho_I &= \left[\frac{2\pi N}{|\mathbf{b}|}\right][\epsilon_i K + D_i Z_{iI} c_i - D_v Z_{vI}(c_v - \bar{c}_{vI})] , \\
\partial_t \rho_V &= \frac{1}{|\mathbf{b}| r_V^0}\{\epsilon_v K - \rho_V [D_i Z_{iV} c_i - D_v Z_{vV}(c_v - \bar{c}_{vV})]\} ,
\end{aligned}
\tag{1}
$$

where $c_v$ corresponds to the vacancy concentration and $c_i$ to that of interstitials. $\rho_N$ is the network dislocation density, $\rho_V$ the vacancy loop, and $\rho_I$ the interstitial loop density. $K$ is the displacement damage rate, $\epsilon_i K$ the interstitial loops production rate, and $\epsilon_v$ the cascade collapse efficiency; $\alpha$ is the recombination coefficient, $\mathbf{b}$ the Burgers vector, $r_V^0$ the mean vacancy loop radius, and $Z\cdots$ are the bias factors which will be approximated by $Z_{iN}=1+B$, $Z_{iI}\cong Z_{iV}=1+B'$, and $Z_{vI}=Z_{vN}=Z_{vV}=1$. $B$ is the excess network bias and $B'$ is the excess loop bias ($B'>B$). $\bar{c}_{vN}$, $\bar{c}_{vV}$, and $\bar{c}_{vI}$ are the concentrations of thermally emitted vacancies from network dislocations, vacancy, and interstitial loops, respectively.

We shall now use the following scaling relations:

$$
\begin{aligned}
&\lambda_v = D_v Z_{vN}\rho_N , \quad \bar{D} = D/\lambda_v , \quad \alpha/\lambda_v = \gamma , \quad P = \gamma K/\lambda_v , \\
&\rho_{V,I}^* = \frac{\rho_{V,I}}{\rho_N} , \quad x_{i,v} = \gamma c_{i,v} , \quad \bar{x}_{vV} \simeq \bar{x}_{vI} = \bar{x}_{vL} , \\
&\mu = \frac{Z_{iN} D_i}{Z_{vN} D_v} = (1+B)\frac{D_i}{D_v} , \quad \tau_V = b r_v^0 \rho_N \gamma , \quad \tau = \lambda_v t , \\
&\tau_I = \frac{b\alpha\rho_N}{2\pi N D_v} .
\end{aligned}
\tag{2}
$$

Equation (1) can now be written in dimensionless form,

$$
\begin{aligned}
\partial_\tau x_i &= P(1-\epsilon_i) - x_i x_v + \bar{D}_i \nabla^2 x_i - \mu x_i (1+\rho_V^* + \rho_I^*) , \\
\partial_\tau x_v &= P(1-\epsilon_v) - x_i x_v + \bar{D}_v \nabla^2 x_v \\
&\quad - (x_v - \bar{x}_{vN}) - (x_v - \bar{x}_{vL})\rho_V^* - (x_v - \bar{x}_{vL})\rho_I^* , \\
\tau_I \partial_\tau \rho_I^* &= \epsilon_i P + \mu(1+\Delta B) x_i - (x_v - \bar{x}_{vL}) , \\
\tau_V \partial_\tau \rho_V^* &= \epsilon_v P - \rho_V^* [\mu(1+\Delta B) x_i - (x_v - \bar{x}_{vL})] .
\end{aligned}
\tag{3}
$$

As in Ref. 12, Eqs. (3) are derived from Eq. (1), on using the approximations $B' \simeq B$ in point defect equations, and $(1+B')/(1+B) \simeq 1+B'-B-BB' \simeq 1+\Delta B$ in the interstitial loop equation, where $\Delta B$ is the difference between the loop and network bias. Since the point defect densities evolve much more rapidly than the loops, they may, as usual, be adiabatically eliminated from the dynamics and their evolution related to that of the loop densities via the following relations:

$$
\begin{aligned}
&\mu x_i^0 - (x_v^0 - \bar{x}_{vL}) = \frac{\bar{\epsilon}P + \Delta}{A_0} , \\
&x_i^0 = -\frac{1}{2}\left\{A_0 + \bar{x}_{vL} - \frac{\bar{\epsilon}P+\Delta}{A_0} - \left[\left[A_0 + \bar{x}_{vL} - \frac{\bar{\epsilon}P+\Delta}{A_0}\right]^2 + 4\frac{P(1-\epsilon_i)}{\mu}\right]^{1/2}\right\} ,
\end{aligned}
\tag{4}
$$

where $\Delta = \bar{x}_{vL} - \bar{x}_{vN}$, $\bar{\epsilon} = \epsilon_v - \epsilon_i$, and $A_0 = 1+\rho_V^0+\rho_I^0$.

The resulting reduced loop dynamics are then given by

$$
\begin{aligned}
\tau_I \partial_\tau \rho_I^0 &= \epsilon_i P + \mu \Delta B x_i^0 + \frac{\bar{\epsilon}P+\Delta}{1+\rho_V^0+\rho_I^0} , \\
\tau_V \partial_\tau \rho_V^0 &= \epsilon_v P - \left[\mu \Delta B x_i^0 + \frac{\bar{\epsilon}P+\Delta}{1+\rho_V^0+\rho_I^0}\right]\rho_V^0 .
\end{aligned}
\tag{5}
$$

Since $A_0$ is continuously increasing in time, one may expect that, after a short transient, $x_i^0$ tends to $P(1-\epsilon_i)/\mu A_0$, even for annealed materials at low temperatures. In other words, the recombination of point defects should not affect the long time evolution of the system.

Numerical solutions of Eqs. (4) and (5) for the parameters of annealed nickel, taken from Ref. 12, are shown in

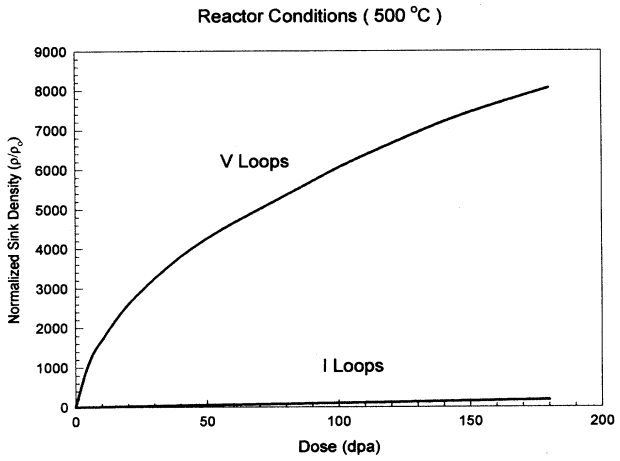


FIG. 3. Evolution of the uniform sink densities of vacancy and interstitial clusters under reactor irradiation conditions ($K=10^{-6}$ dpa/s, $T=500$ °C) for well-annealed nickel ($\rho_N=10^{13}$ m$^{-2}$). Defect parameters are taken from Ref. 12.

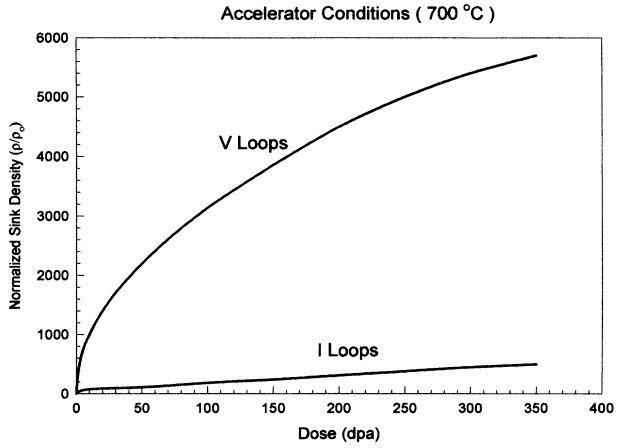


FIG. 4. Evolution of the uniform sink densities of vacancy and interstitial clusters under typical accelerator conditions ($K=10^{-3}$ dpa/s, $T=700$ °C) for well-annealed nickel ($\rho_N=10^{13}$ m$^{-2}$). Defect parameters are taken from Ref. 12.

Fig. 3 for typical conditions of reactor irradiation at $K=10^{-6}$ dpa/s and $T=500$ °C. On the other hand, dislocation loop densities at higher temperatures (700 °C) and higher displacement damage rate ($10^{-3}$ dpa/s) typical of ion irradiation, are shown in Fig. 4.

## III. DISLOCATION LOOP DYNAMICS

To study the evolution of nonuniform defect distributions and the eventual occurrence of microstructure formation, we also need to derive the evolution equations of the inhomogeneous perturbations of the uniform state. These perturbations are defined as

$$\delta x_i = x_i - x_i^0, \quad \delta x_v = x_v - (x_v^0 - \bar{x}_{vL}) ,$$
$$\delta\rho_V = \frac{\rho_V^* - \rho_V^0}{\rho_V^0}, \quad \delta\rho_I = \frac{\rho_I^* - \rho_I^0}{\rho_I^0} . \tag{6}$$

Let us introduce these variables in the system (3), and consider first the corresponding evolution equations for the Fourier components (of wave vectors $\mathbf{q}$) of point defect perturbations. Since point defect concentrations evolve much more rapidly than loop concentrations, they may be adiabatically eliminated. On separating the linear and nonlinear parts of their evolution, one easily sees that point defect perturbations obey the following equations:

$$\delta x_{i,q} = -\frac{1}{\Delta_q}\left[\alpha_q(\rho_V^0\delta\rho_{Vq}+\rho_I^0\delta\rho_{Iq}) + \int dk(\beta_q\delta x_{i,q-k}+\gamma_q\delta x_{v,q-k}) \times(\rho_V^0\delta\rho_{Vk}+\rho_I^0\delta\rho_{Ik}) + \int dk\,\mu A_{Vq}\delta x_{i,q-k}\delta x_{v,k}\right] ,$$
$$\delta x_{v,q} = -\frac{1}{\Delta_q}\left[\epsilon_q(\rho_V^0\delta\rho_{Vq}+\rho_I^0\delta\rho_{Iq}) + \int dk(\mu_q\delta x_{i,q-k}+\nu_q\delta x_{v,q-k}) \times(\rho_V^0\delta\rho_{Vk}+\rho_I^0\delta\rho_{Ik}) + \int dk\,\mu A_{Iq}\delta x_{i,q-k}\delta x_{v,k}\right] , \tag{7}$$

where

$$\Delta_q = \mu A_{Vq} A_{Iq} + x_v^0 A_{Vq} + \mu x_i^0 A_{Iq} ,$$
$$\alpha_q = \mu x_i^0 A_{Vq} + x_i^0 \frac{\bar{\epsilon}P+\Delta}{A_0} ,$$

$$\beta_q = \mu(A_{Vq}+x_i^0), \quad \gamma_q = -x_i^0 ,$$
$$\epsilon_q = \mu A_{Iq}(x_v^0 - \bar{x}_{vL}) - x_v^0\frac{\bar{\epsilon}P+\Delta}{A_0} ,$$
$$\mu_q = -x_v^0, \quad \nu_q = \mu A_{Iq} + x_v^0, \quad A_0 = 1+\rho_V^0+\rho_I^0 ,$$
$$A_{Vq} = A_0 + q^2\bar{D}_v, \quad A_{Iq} = A_0 + \frac{q^2\bar{D}_v}{1+B} . \tag{8}$$

In the preceding section, we showed that point defect recombination does not affect the long time behavior of the system. Hence, the various coefficients which appear into Eq. (7) may be approximated by their values in the sink dominated regime, which are obtained by taking the dominant contributions in $A_0$, $A_{Vq}$ and $A_{Iq}$. This leads to

$$\delta x_{i,q} = -\frac{P(1-\epsilon_i)}{\mu A_0 A_{Iq}}(\rho_V^0 \delta\rho_{Vq} + \rho_I^0 \delta\rho_{Iq}) - \int dk \frac{1}{A_{Iq}} \delta x_{i,k}(\rho_V^0 \delta\rho_{Vq-k} + \rho_I^0 \delta\rho_{Iq-k}) ,$$
$$\delta x_{v,q} = -\frac{P(1-\epsilon_v)-\Delta}{A_0 A_{Vq}}(\rho_V^0 \delta\rho_{Vq} + \rho_I^0 \delta\rho_{Iq}) - \int dk \frac{1}{A_{Vq}} \delta x_{v,k}(\rho_V^0 \delta\rho_{Vq-k} + \rho_I^0 \delta\rho_{Iq-k}) . \quad (9)$$

Point defect perturbations may thus be obtained from Eq. (9) by an iterative procedure and expressed as an expansion in powers of the loop density perturbations, resulting in the following vector form for the perturbations:

$$\delta \mathbf{x}_q = \Sigma_{n\geq 1} \int dk \cdots \int dk_{n-1} \overline{\overline{D}}^{(n)}_{q,\ldots,k_{n-1}} \times \mathbf{T}_q \delta\rho_{q-k} \cdots \delta\rho_{k_{n-1}} , \quad (10)$$

where

$$\overline{\overline{D}}^{(n)}_{q,\ldots,k_{n-1}} = \left[ \frac{(-1)^n}{A_{Iq} \cdots A_{Ik_{n-1}}}, 0; 0, \frac{(-1)^n}{A_{Vq} \cdots A_{Vk_{n-1}}} \right]$$

and $\delta \mathbf{x}_q = (\delta x_{i,q}, \delta x_{v,q})$. Details of the derivation for Eq. (10) are given in Appendix A.

On the other hand, the evolution of loop density perturbations is given by

$$\tau_V \partial_\tau \delta\rho_{Vq} = -\frac{\epsilon_v P}{\rho_V^0} \delta\rho_{Vq} - [\mu(1+\Delta B)\delta x_{iq} - \delta x_{vq}] - \int dk \, \delta\rho_{Vq-k}[\mu(1+\Delta B)\delta x_{ik} - \delta x_{vk}] , \quad (11)$$
$$\tau_I \partial_\tau \delta\rho_{Iq} = -\bar{\epsilon}_i P \frac{\delta\rho_{Iq}}{\rho_I^0} + [\mu(1+\Delta B)\delta x_{iq} - \delta x_{vq}] \frac{1}{\rho_I^0} ,$$

with $\bar{\epsilon}_i = \epsilon_i + [\bar{\epsilon} + \Delta/P + (1-\epsilon_i)\Delta B]/A_0$.

Equations (11) can also be put in the following vectorial form:

$$\overline{\overline{\tau}} \partial_t \overline{\Lambda}_q = \overline{\overline{L}}_q \overline{\Lambda}_q + \Sigma_{n\geq 1} \int dk_1 \cdots \times \int dk_n \overline{\overline{M}}_n \overline{\Lambda}_{q-k_1} \delta\rho_{k_1-k_2} \cdots \delta\rho_{k_n} . \quad (12)$$

Details of derivations are left to Appendix B. Equation (12) describes the evolution dynamics in two parts. The first term on the right-hand side represents the linear evolution matrix, while the second term describes the nonlinear regime. It is to be noted here that the vector $\overline{\Lambda}$ is a linear combination of loop density perturbations. Other terms are explained in Appendix B.

## IV. THE LINEAR STABILITY ANALYSIS

The stability of the uniform dislocation densities may be analyzed through the linear part of the evolution equation (12) for their inhomogeneous perturbations. However, the elements of the corresponding evolution matrix are time dependent, and this situation prevents us from performing the usual stability analysis. Nevertheless, some insight into the behavior of the system may be obtained within the quasistatic approximation, i.e., when the stability of the uniform densities is evaluated by considering them as frozen or stationary at each moment. One thus expects an instability when at least one eigenvalue of the evolution matrix acquires a positive real part. Of course, this approximation does not describe correctly the growth rate of the perturbations, but in similar problems, it seems to predict the instability threshold quite accurately.[18] Since one eigenvalue of the linear evolution matrix becomes positive when

$$\Gamma_q \geq \frac{\epsilon_v P}{(\rho_V^0)^2 - \epsilon_v \rho_I^0/\bar{\epsilon}_i} \quad (13)$$

the instability threshold is obtained when the maximum of $\Gamma_q$ reaches $\epsilon_v P/[(\rho_V^0)^2 - \epsilon_v \rho_I^0/\bar{\epsilon}_i]$. This maximum is given by the condition

$$\frac{A_0 + q_c^2 \bar{D}_V}{A_0 + q_c^2 \bar{D}_V/(1+B)} = \left[ \frac{(1-\epsilon_v - \Delta/P)(1+B)}{(1-\bar{\epsilon}_i)(1+\Delta B)} \right]^{1/2} = Q \quad (14)$$

which defines the critical wave number as

$$q_c^2 = \frac{A_0(Q-1)(1+B)}{\bar{D}_V(1+B-Q)} \simeq \frac{A_0(B-\epsilon')}{\bar{D}_V(B+\epsilon')} \sqrt{(1+B)} , \quad (15)$$

with $\epsilon' = \epsilon_v - \bar{\epsilon}_i + \Delta B + (\Delta + \Delta B)/P$. This leads to the following instability threshold for the bifurcation parameter $\rho_V^0/A_0$:

$$\left. \frac{\rho_V^0}{A_0} \right|_c = 2 \left[ \frac{\epsilon_v B}{1-\bar{\epsilon}_i} \right]^{1/2} \frac{1}{B+\epsilon'} , \quad (16)$$

which is an obvious generalization of the result obtained in Ref. (12) in the absence of interstitial loop production rate $\epsilon_i$.

When $\epsilon_v/\epsilon' < 1$, i.e., when $\bar{\epsilon}_i < \Delta B + \Delta/P$, one obtains, by straightforward dimensional analysis, a similar relationship between vacancy and interstitial loop densities than the one obtained in Ref. 12, namely,

$$\rho_V^0 \cong \frac{\epsilon_v}{\epsilon' - \epsilon_v}(1+\rho_I^0)$$

and the quasi-steady-state uniform dislocation densities for clustered defects follow a $\sqrt{\tau}$ time dependence, after transients related to either interstitial loop nucleation, since their time dependence is given by

$$\rho_I^0=\sqrt{1+\eta\tau}-1\ ,$$
$$\rho_V^0=\left[\frac{\epsilon_v}{\epsilon'-\epsilon_v}\right]\sqrt{1+\eta\tau}\ ,$$

where $\eta=2P(\epsilon'-\epsilon_v)\tau_I$.

Hence the bifurcation parameter tends, in the asymptotic time limit, to $\epsilon_v/\epsilon'$, and instability occurs if

$$\frac{\epsilon_v}{\epsilon'}>2\left[\frac{\epsilon_v}{1-\bar{\epsilon}_i}\right]^{1/2}\frac{1}{B+\epsilon'}\ . \tag{17}$$

In the other case, i.e., when $\bar{\epsilon}_i>\Delta B+\Delta/P$, and since $\tau_I\gg\tau_V$, the uniform dislocation densities follow a linear time growth $[\rho_I^0\rightarrow(\bar{\epsilon}_iP/\tau_I)$ and $\rho_V^0\rightarrow\{[(\bar{\epsilon}_i-\Delta B)P-\Delta]/\tau_V\}t]$ and the bifurcation parameter tends to 1. When the system is dominated by vacancy loops, the instability occurs if

$$2\left[\frac{\epsilon_v}{1-\bar{\epsilon}_i}\right]^{1/2}\frac{1}{B+\epsilon'}<1\ . \tag{18}$$

## V. THE WEAKLY NONLINEAR REGIME

Close to the instability threshold, space-time separation occurs between stable and unstable modes, the characteristic scales of the latter being by far the largest. The stable modes may thus be adiabatically eliminated, and the dynamics reduced to the weakly nonlinear unstable modes dynamics, which governs the long time evolution of the system and captures the asymptotic properties of the complete kinetic model in the vicinity of its bifurcation point. In order to perform this adiabatic elimination, one has first to diagonalize the loop dynamics and to separate stable and unstable modes. This leads to the following evolution equations for the stable $\Sigma_q$ and unstable $\sigma_q$ modes:

$$\bar{\bar{\tau}}\partial_t\bar{\sigma}_q=\bar{\bar{\Omega}}_q\bar{\sigma}_q+\Sigma_{n\geq1}(-1)^{n-1}\int dk_1\cdots\int dk_n\bar{\bar{N}}_n\bar{\sigma}_{q-k_1}(\Pi_{i=1}^{n-1}\delta\bar{\rho}_{k_i-k_{i+1}})\delta\bar{\rho}_{k_n}\ , \tag{19}$$

where, at the leading order in $(\rho_V^0)^{-1}$, and close to the bifurcation point, one has

$$\bar{\sigma}_q=\begin{bmatrix}\sigma_q\\ \Sigma_q\end{bmatrix}=\bar{\bar{D}}\begin{bmatrix}\delta\rho_{Vq}\\ \delta\rho_{Iq}\end{bmatrix}=\begin{bmatrix}1 & b\\ c & 1\end{bmatrix}\begin{bmatrix}\delta\rho_{Vq}\\ \delta\rho_{Iq}\end{bmatrix}\ ,$$
$$\bar{\bar{\Omega}}_q=\begin{bmatrix}\omega_\sigma(q) & 0\\ 0 & \omega_\Sigma(q)\end{bmatrix}\ ,$$
$$\bar{\bar{N}}_n=\begin{bmatrix}\Gamma^{(n)}\rho_V^0\alpha\beta+\Gamma^{(n-1)} & \Gamma^{(n)}\rho_I^0\gamma\beta-\Gamma^{(n-1)}\dfrac{\epsilon_v(\rho_I^0)^2}{\epsilon_i(\rho_V^0)^2}\dfrac{\tau_I}{\tau_V}\\ -\Gamma^{(n)}\dfrac{\rho_V^0}{\rho_I^0}\alpha\delta-\Gamma^{(n-1)}\dfrac{\epsilon_v}{\epsilon_i\rho_V^0} & -\Gamma^{(n)}\rho_I^0\gamma\delta-\Gamma^{(n-1)}\dfrac{\epsilon_v^2(\rho_I^0)^2}{\epsilon_i^2(\rho_V^0)^2}\dfrac{\tau_I}{\tau_V}\end{bmatrix} \tag{20}$$

$$\delta\bar{\rho}_k=\rho_V^0\sigma_k+\rho_I^0\Sigma_k\ ,$$

with

$$b=\frac{\epsilon_v(\rho_I^0)^2}{\epsilon_i(\rho_V^0)^2}\frac{\tau_I}{\tau_V},\quad c=\frac{\epsilon_v}{\epsilon_i\rho_V^0}\frac{\tau_V}{\tau_I}\ ,$$
$$\omega_\sigma(q)=\left[\Gamma_q\left[\rho_V^0-\frac{\epsilon_v\rho_I^0}{\epsilon_i\rho_V^0}\right]-\frac{\epsilon_vP}{\rho_V^0}\right]\ ,$$
$$\omega_\Sigma(q)=-\frac{\epsilon_iP}{\rho_I^0},\quad \alpha=1-c\frac{\rho_I^0}{\rho_V^0}=1-\frac{\epsilon_v\rho_I^0}{\epsilon_i(\rho_V^0)^2}\frac{\tau_V}{\tau_I}\ , \tag{21}$$
$$\beta=1-b\frac{\tau_V}{\tau_I\rho_I^0}=1-\frac{\epsilon_v\rho_I^0}{\epsilon_i(\rho_V^0)^2}$$
$$\gamma=1-b\frac{\rho_V^0}{\rho_I^0}=1-\frac{\epsilon_v\rho_I^0}{\epsilon_i\rho_V^0}\frac{\tau_I}{\tau_V}$$
$$\delta=1-c\frac{\tau_I\rho_I^0}{\tau_V}=1-\frac{\epsilon_v\rho_I^0}{\epsilon_i\rho_V^0}\ .$$

Hence, at the bifurcation point, the modes $\sigma_q$ become unstable while the modes $\Sigma_q$ remain stable. Furthermore, the time-scale separation between these two classes of modes allows the adiabatic elimination of the stable modes $\Sigma_q$. This may be done as usual[12,16,17] on solving the evolution equation for $\Sigma_q$ after neglecting its time derivative and expressing it as a series expansion in powers of the $\sigma_q$ at $q_c$. In Appendix C, the inverse Fourier transform of Eq. (19) is derived to give the following evolution equation for $\sigma$:

$$\tau_0\partial_t\sigma(\mathbf{r},t)=\left[\frac{b-b_c}{b_c}-\xi_0^2(\nabla^2+q_c^2)^2\right]\sigma(\mathbf{r},t)$$
$$+v\sigma(\mathbf{r},t)^2-u\sigma(\mathbf{r},t)^3\ , \tag{22}$$

where

$$
\begin{aligned}
b_c &= 2\left[\frac{\epsilon_v B}{1-\bar{\epsilon}_i}\right]^{1/2}\frac{1}{B+\epsilon'}\,, \\
\xi_0^2 &= \frac{b_c}{8}\left[\frac{\bar{D}_v}{A_0}\right]^2\left[\frac{B+\epsilon'}{B}\right]^2\,, \\
\tau_0 &= \tau_V\bar{\tau} = \tau_V\frac{(\epsilon'+2B)^2}{\epsilon_v PB(B+\epsilon')}\,, \\
v &= \frac{(\epsilon'+2B)^2}{\rho_V^0 B(\epsilon'+B)}(1+\rho)\,, \\
u &= \frac{(\epsilon'+2B)^2}{\rho_V^0 B(\epsilon'+B)}\rho\left[1+\tfrac{3}{4}\rho+\frac{\epsilon_v}{\bar{\epsilon}_i}(1+\rho)\right]\,, \\
\rho &= 2\left[\frac{\epsilon_v}{B(1-\bar{\epsilon}_i)}\right]^{1/2}\,.
\end{aligned}
\tag{23}
$$

Hence, the conclusions of our previous analysis are not qualitatively modified, but only quantitatively. We remain with the general results of bifurcation theory leading to the fact that the following structures may be selected:[18]

(1) bcc lattices or filamental structures of cubic symmetry, associated with a subcritical bifurcation and described by the following amplitude equation:

$$
\begin{aligned}
\tau_0\partial_t A_i = &\left[\frac{b-b_c}{b_c}-4(\mathbf{q}_i\cdot\nabla)^2\right]A_i+v\Sigma_{j,k}\bar{A}_j\bar{A}_k \\
&-3uA_i(|A_i|^2+2\Sigma_{j\neq i}|A_j|^2)\,,
\end{aligned}
\tag{24}
$$

with $i,j,k=1,\ldots,6$, $\mathbf{q}_i+\mathbf{q}_j+\mathbf{q}_k=0$, $|\mathbf{q}_i|=q_c$, and $\sigma=\Sigma_i(A_i e^{i\mathbf{q}_i\cdot\mathbf{r}}+\text{c.c.})$.

These bcc lattices are stable in the range $-v^2/33u<(b-b_c)/b_c<3v^2/u$.

(2) Rodlike hexagonal or triangular structures also appearing via a first-order-like transition (subcritical bifurcations), are described by the amplitude equation

$$
\begin{aligned}
\tau_0\partial_t A_i = &\left[\frac{b-b_c}{b_c}-4(\mathbf{q}_i\cdot\nabla)^2\right]A_i+v\Sigma_{j,k}\bar{A}_j\bar{A}_k \\
&-3uA_i(|A_i|^2+2\Sigma_{j\neq i}|A_j|^2)\,,
\end{aligned}
\tag{25}
$$

with $i,j,k=1,\ldots,3$, $\mathbf{q}_i+\mathbf{q}_j+\mathbf{q}_k=0$, $|\mathbf{q}_i|=q_c$, and $\sigma=\Sigma_i(A_i e^{i\mathbf{q}_i\cdot\mathbf{r}}+\text{c.c.})$, and are stable in the range $-v^2/15u<(b-b_c)/b_c<v^2/u$.

(3) Wall structures corresponding to the spatial modulations of the loop densities in one direction. They appear via a second-order-like transition, or supercritical bifurcation, and are described by the following amplitude equation:

$$
\tau_0\partial_t A=\left[\frac{b-b_c}{b_c}+4(\mathbf{q}_i\nabla+\cdots)^2\right]A-3uA|A|^2 \tag{26}
$$

and are only stable in the range $v^2/3u<(b-b_c)/b_c$.

In the present case, the interstitial production rate $\epsilon_i P$ leads to an increase of the instability threshold, since

$$
b_c = 2\left[\frac{\epsilon_v}{1-\bar{\epsilon}_i}\right]^{1/2}\frac{1}{B+\epsilon'}\,, \tag{27}
$$

and may thus eventually suppress the transition.

On the other hand, as discussed in Ref. 12, the stability region of bcc microstructure is still shrinking with dose, or with time, since $v^2/u$ remains proportional to $(\rho_V^0)^{-1}$, which is decreasing with time. Hence, if the interstitial production rate does not suppress the transition, the three-dimensional (3D) bcc microstructure still appears as a transient state, and the planar wall structure remains the final state of the microstructure in this evolution model, as may be inferred from the dose dependence of the bifurcation diagram as shown in Figs. 5–7. The evolution of the critical wavelength with dose under accelerator conditions is shown in Fig. 8. The wavelength is normalized to that at the start of irradiation, where the value can be found in Ref. 26. The wavelength is shown to decrease as a function of irradiation dose. For example, under annealed conditions the wavelength is reduced to about one-third of its original value by a dose of 10 dpa.

## VI. CONCLUSIONS AND DISCUSSION

We presented here a dynamical analysis of microstructure formation and evolution in irradiated metals and alloys based on the most complete set of kinetic equations at hand for the description of interacting point (interstitials and vacancies) and line defects (vacancy and interstitial loops). A previous analysis[12] along these lines was based on a reaction-diffusion model taking into account the basic elements of defect dynamics, namely, point defect creation, recombination, and migration to microstructures. In the present analysis, we furthermore explicitly considered direct loop production via cascades for

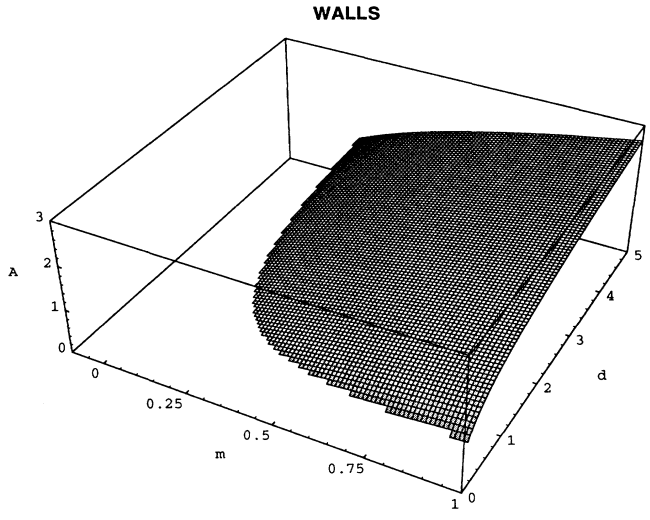


FIG. 5. Stability surface for wall structures in the amplitude ($A$), distance to threshold ($m$), and irradiation dose ($d$) space (in reduced units: e.g., for annealed steel under reactor conditions with $K=10^{-6}$ dpa/s, $T=500$ °C, $m=4$ and $d=1$ correspond to 0.1 dpa).

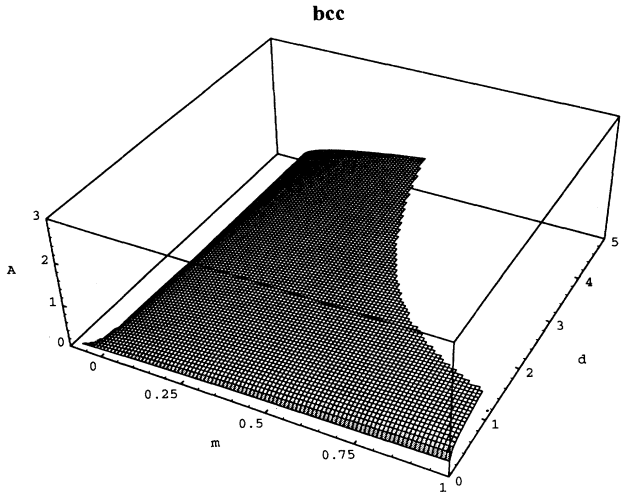


FIG. 6. Stability surface for bcc structures in the amplitude ($A$), distance to threshold ($m$), and irradiation dose ($d$) space (in reduced units: e.g., for annealed steel under reactor conditions with $K=10^{-6}$ dpa/s, $T=500$ °C, $m=4$ and $d=1$ corresponds to 0.1 dpa). One sees that at fixed $m$ the bcc structure always becomes unstable versus wall structures at sufficiently high dose.

both vacancy and interstitial loops. We also obtained a compact formulation of the weakly nonlinear dynamics close to the pattern-forming instability in the quasi-steady-state approximation.

We showed that defect recombination does not affect the long time evolution of the system, and hence, does not affect the properties of the emerging microstructure. On the other hand, direct interstitial loop production increases the critical value of the bifurcation parameter and tends to stabilize uniform defect distributions. The previous comparisons with experimental observations, namely, the existence of clusters of cubic symmetry,[19,20] defect walls,[21,22] as well as anisotropic arrangements of planar aggregates of defects,[23–25] are not qualitatively affected in the present description. It is also confirmed that dominant vacancy loop cascades are necessary for the formation of 3D periodic microstructure. In such cases (for example, in stainless steel or nickel irradiated under typical reactor conditions), the effective bifurcation parameter still increases with time or irradiation dose, and, after an initial phase where loop clustering should occur in the form of bcc lattices, the system should finally reach a planar wall structure, even for isotropic defect mobilities. These structures could then be in nonparallel orientations, i.e., with a structure different from the structure of the host lattice. This behavior, which seems consistent with many experimental observations, also occurs under accelerator conditions, particularly for an initially annealed microstructure. For heavily cold worked initial microstructure, or dominant interstitial loop cascades, the bifurcation parameter may not be able to reach the instability threshold. However, since bcc structures may appear subcritically, 3D loop clustering could occur transitorily, but the final defect distributions should be uniform.

Hence, since the symmetry of the defect structures is a crucial issue in irradiated materials, the present discussion shows that a careful study of the postbifurcation regime is needed to test the relevance of particular kinetic models to the interpretation of experimental observations. Furthermore, we emphasize here the importance of performing systematic experimental studies on the

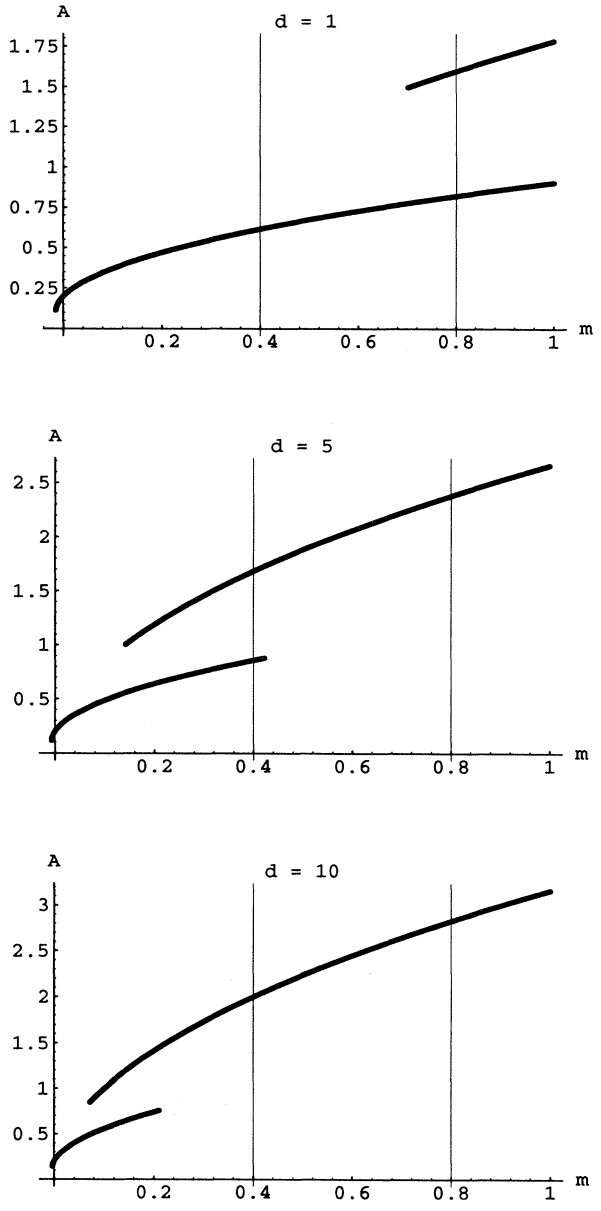


FIG. 7. Cuts in the stability surface of wall (upper curves) and bcc (lower curves) structures at increasing irradiation dose ($d$), showing as in Figs. 5 and 6 that, at fixed $m$, the bcc structure always becomes unstable versus wall structures at sufficiently high dose.

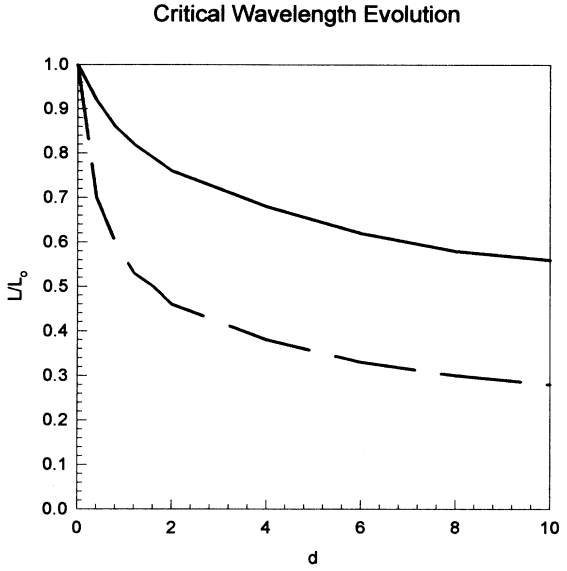


FIG. 8. Evolution of the reduced critical wavelength ($L=l/l_0$) with time (in reduced units) for cold worked (upper curve) and annealed (lower curve) conditions. The values of $l_0$ will depend on chosen parameters from Ref. 26.

temporal evolution of 3D periodic arrangements of defect clusters.[11] In the experimental investigations of Jaeger, Ehrhart, and Schilling, a scenario similar to our predictions is observed. Blocks or agglomerates of defect clusters along cubic axes were observed to disappear at higher doses in favor of planar walls parallel to {110} matrix planes in Cu and Ni, and up to a dose of 4 dpa. No competing arrangement of higher stability than planar walls was observed. On the other hand, numerical analysis of the kinetic model discussed here is also needed to confirm and extend the results of the weakly nonlinear analysis presented here. Significant progress may be expected in understanding, and predicting the effects of materials instabilities on the macroscopic behavior of driven or degrading solids can be achieved, by the combination of bifurcation analysis, amplitude equation description, numerical simulations, and carefully devised experiments.

## ACKNOWLEDGMENTS

Financial assistance through Grant No. SC1*-CT092-0006 of the Commission of the European Community and through NATO Grant No. CRG-931365 is gratefully acknowledged. The support of the Office of Fusion Energy (OFE) of the U.S. Department of Energy (DOE) through Grant No. DE-FG03-84ER52110 with U.C.L.A. is also acknowledged.

## APPENDIX A

Substitution of successive approximations to point defect perturbations in terms of ascending powers of loop density perturbations gives

$$\delta x_{i,q}=-\frac{P(1-\epsilon_i)}{\mu A_0 A_{Iq}}(\rho_V^0\delta\rho_{Vq}+\rho_I^0\delta\rho_{Iq})+\int dk\frac{P(1-\epsilon_i)}{\mu A_0 A_{Iq}A_{Ik}}(\rho_V^0\delta\rho_{Vk}+\rho_I^0\delta\rho_{Ik})(\rho_V^0\delta\rho_{Vq-k}+\rho_I^0\delta\rho_{Iq-k})$$
$$-\int dk\int dk'\frac{P(1-\epsilon_i)}{\mu A_0 A_{Iq}A_{Ik}A_{Ik'}}(\rho_V^0\delta\rho_{Vk'}+\rho_I^0\delta\rho_{Ik'})(\rho_V^0\delta\rho_{Vk-k'}+\rho_I^0\delta\rho_{Ik-k'})(\rho_V^0\delta\rho_{Vq-k}+\rho_I^0\delta\rho_{Iq-k})+\cdots \tag{A1}$$
$$\delta x_{v,q}=-\frac{P(1-\epsilon_v)-\Delta}{A_0 A_{Vq}}(\rho_V^0\delta\rho_{Vq}+\rho_I^0\delta\rho_{Iq})+\int dk\frac{P(1-\epsilon_v)-\Delta}{A_0 A_{Vq}A_{Vk}}(\rho_V^0\delta\rho_{Vk}+\rho_I^0\delta\rho_{Ik})(\rho_V^0\delta\rho_{Vq-k}+\rho_I^0\delta\rho_{Iq-k})$$
$$-\int dk\int dk'\frac{P(1-\epsilon_v)-\Delta}{A_0 A_{Vq}A_{Vk}A_{Vk'}}(\rho_V^0\delta\rho_{Vk'}+\rho_I^0\delta\rho_{Ik'})(\rho_V^0\delta\rho_{Vk-k'}+\rho_I^0\delta\rho_{Ik-k'})(\rho_V^0\delta\rho_{Vq-k}+\rho_I^0\delta\rho_{Iq-k})+\cdots ,$$

or

$$\delta x_{i,q}=-\frac{P(1-\epsilon_i)}{\mu A_0 A_{Iq}}\left[(\rho_V^0\delta\rho_{Vq}+\rho_I^0\delta\rho_{Iq})+\int dk\frac{1}{A_{Ik}}(\rho_V^0\delta\rho_{Vk}+\rho_I^0\delta\rho_{Ik})(\rho_V^0\delta\rho_{Vq-k}+\rho_I^0\delta\rho_{Iq-k})\right.$$
$$-\int dk\int dk'\frac{1}{A_{Ik}A_{Ik'}}(\rho_V^0\delta\rho_{Vk'}+\rho_I^0\delta\rho_{Ik'})$$
$$\left.\times(\rho_V^0\delta\rho_{Vk-k'}+\rho_I^0\delta\rho_{Ik-k'})(\rho_V^0\delta\rho_{Vq-k}+\rho_I^0\delta\rho_{Iq-k})+\cdots\right],$$
$$\delta x_{v,q}=-\frac{P(1-\epsilon_v)-\Delta}{A_0 A_{Vq}}\left[(\rho_V^0\delta\rho_{Vq}+\rho_I^0\delta\rho_{Iq})+\int dk\frac{1}{A_{Vk}}(\rho_V^0\delta\rho_{Vk}+\rho_I^0\delta\rho_{Ik})(\rho_V^0\delta\rho_{Vq-k}+\rho_I^0\delta\rho_{Iq-k})\right. \tag{A2}$$
$$-\int dk\int dk'\frac{1}{A_{Vk}A_{Vk'}}(\rho_V^0\delta\rho_{Vk'}+\rho_I^0\delta\rho_{Ik'})$$
$$\left.\times(\rho_V^0\delta\rho_{Vk-k'}+\rho_I^0\delta\rho_{Ik-k'})(\rho_V^0\delta\rho_{Vq-k}+\rho_I^0\delta\rho_{Iq-k})+\cdots\right],$$

or, in vectorial form

$$\delta \mathbf{x}_q = \left[ \bar{\bar{D}}_q \delta\rho_q + \int dk \bar{\bar{D}}_q \bar{\bar{D}}_k \delta\rho_{q-k} \delta\rho_k + \int dk \int dk' \bar{\bar{D}}_q \bar{\bar{D}}_k \bar{\bar{D}}_{k'} \delta\rho_{q-k} \delta\rho_{k-k'} \delta\rho_{k'} + \cdots \right] \mathbf{T}_q \ , \tag{A3}$$

where $\delta \mathbf{x}_q = (\delta x_{i,q}, \delta x_{v,q})$,

$$\mathbf{T}_q = \left[ \frac{P(1-\epsilon_i)}{\mu A_0}, \ \frac{P(1-\epsilon_v)-\Delta}{A_0} \right], \quad \bar{\bar{D}}_q = \left[ \frac{-1}{A_{Iq}}, 0; 0, \frac{-1}{A_{Vq}} \right],$$

and $\delta\rho_q = \rho_V^0 \delta\rho_{Vq} + \rho_I^0 \delta\rho_{Iq}$.

Since the matrix $\bar{\bar{D}}_q$ is diagonal, Eq. (A3) may be rewritten as

$$\delta \mathbf{x}_q = \Sigma_{n \geq 1} \int dk \cdots \int dk_{n-1} \bar{\bar{D}}^{(n)}_{q, \ldots, k_{n-1}} \mathbf{T}_q \delta\rho_{q-k} \cdots \delta\rho_{k_{n-1}} \ . \tag{A4}$$

## APPENDIX B

The difference between point defect perturbations can be written as

$$\mu(1+\Delta B)\delta x_{iq} - \delta x_{vq} = \Sigma_{n \geq 1} (-1)^n \int dk \cdots \int dk_{n-1} \left[ \frac{P(1-\epsilon_i)}{A_0} \frac{1+\delta B}{A_{Iq} \cdots A_{Ik_{n-1}}} - \frac{P(1-\epsilon_v)-\Delta}{A_0} \frac{1}{A_{Vq} \cdots A_{Vk_{n-1}}} \right] \delta\rho_{q-k} \cdots \delta\rho_{k_{n-1}} \ , \tag{B1}$$

or

$$\mu(1+\Delta B)\delta x_{iq} - \delta x_{vq} = -\Gamma_q \delta\rho_q + \Sigma_{n \geq 1} (-1)^{n-1} \int dk_1 \cdots \int dk_n \Gamma^{(n)}_{q, \ldots, k_n} \delta\rho_{q-k_1} \cdots \delta\rho_{k_n} \ , \tag{B2}$$

with

$$\Gamma_q = \frac{P(1-\epsilon_i)}{A_0} \frac{1+\Delta B}{A_{Iq}} - \frac{P(1-\epsilon_v)-\Delta}{A_0} \frac{1}{A_{Vq}} \tag{B3}$$

and

$$\Gamma^{(n)}_{q, \ldots, k_n} = \frac{P(1-\epsilon_i)}{A_0} \frac{1+\Delta B}{A_{Iq} \cdots A_{Ik_n}} - \frac{P(1-\epsilon_v)-\Delta}{A_0} \frac{1}{A_{Vq} \cdots A_{Vk_n}} \ . \tag{B4}$$

Hence, the linear part of the loop dynamics may be written as

$$\begin{aligned} \tau_V \partial_\tau \delta\rho_{Vq} &= -\left[ \frac{\epsilon_v P}{\rho_V^0} - \rho_V^0 \Gamma_q \right] \delta\rho_{Vq} + \rho_I^0 \Gamma_q \delta\rho_{Iq} \ , \\ \tau_I \partial_\tau \delta\rho_{Iq} &= -\frac{\rho_V^0}{\rho_I^0} \Gamma_q \delta\rho_{Vq} - \left[ \Gamma_q + \frac{\bar{\epsilon}_i P}{\rho_I^0} \right] \delta\rho_{Iq} \ , \end{aligned} \tag{B5}$$

while its nonlinear part is given by

$$\begin{aligned} \tau_V \partial_\tau \delta\rho^{\mathrm{NL}}_{Vq} &= \Sigma_{n \geq 1} (-1)^{n-1} \int dk_1 \cdots \int dk_n [\Gamma^{(n)}_{q, \ldots, k_n} \delta\rho_{q-k_1} + \Gamma^{(n-1)}_{k_1, \ldots, k_n} \delta\rho_{V, q-k_1}] \delta\rho_{k_1-k_2} \cdots \delta\rho_{k_n} \ , \\ \tau_I \partial_\tau \delta\rho^{\mathrm{NL}}_{Iq} &= -\Sigma_{n \geq 1} \frac{(-1)^{n-1}}{\rho_I^0} \int dk_1 \cdots \int dk_n \Gamma^{(n)}_{q, \ldots, k_n} \delta\rho_{q-k_1} \cdots \delta\rho_{k_n} \end{aligned} \tag{B6}$$

[note that $\Gamma^{(0)}_k = \Gamma_k$; cf. (B3)].

Hence, the loop dynamics may be cast in the vectorial form,

$$\bar{\bar{\tau}} \partial_t \bar{\Lambda}_q = \bar{\bar{L}}_q \bar{\Lambda}_q + \Sigma_{n \geq 1} \int dk_1 \cdots \int dk_n \bar{\bar{M}}_n \bar{\Lambda}_{q-k_1} \delta\rho_{k_1-k_2} \cdots \delta\rho_{k_n} \ , \tag{B7}$$

where

$$\bar{\bar{\tau}}=\begin{bmatrix}\tau_V & 0\\ 0 & \tau_I\end{bmatrix},\quad \bar{\Lambda}_q=\begin{bmatrix}\delta\rho_{Vq}\\ \delta\rho_{Iq}\end{bmatrix}$$

$$\bar{\bar{L}}_q=\begin{bmatrix}-\frac{\epsilon_v P}{\rho_V^0}+\rho_V^0\Gamma_q & \rho_I^0\Gamma_q\\ -\frac{\rho_V^0}{\rho_I^0}\Gamma_q & -\Gamma_q-\frac{\bar{\epsilon}_i P}{\rho_I^0}\end{bmatrix}, \tag{B8}$$

$$\bar{\bar{M}}_n=(-1)^{n-1}\begin{bmatrix}\Gamma^{(n)}_{q,\ldots,k_n}\rho_V^0+\Gamma^{(n-1)}_{k_1,\ldots,k_n} & \Gamma^{(n)}_{q,\ldots,k_n}\rho_I^0\\ \Gamma^{(n)}_{q,\ldots,k_n}\frac{\rho_V^0}{\rho_I^0} & -\Gamma^{(n)}_{q,\ldots,k_n}\end{bmatrix},$$

where

$$\delta\rho_k=\rho_V^0\delta\rho_{Vk}+\rho_I^0\delta\rho_{Ik}\ .$$

## APPENDIX C

The stable modes $\Sigma_q$ are expressed by an iterative solution in powers of $\sigma_q$ and $q_c$, resulting in the following equation:

$$\Sigma_q=-\frac{1}{\omega_\Sigma(q_c)}\Sigma_{n\geq 1}(-1)^{n-1}\int dk_1\cdots\int dk_n[(\bar{\bar{N}}_n(q_c))_{21}\sigma_{q-k_1}+(\bar{\bar{N}}_n(q_c))_{22}\Sigma_{q-k_1}](\Pi_{i=1}^{n-1}\delta\bar{\rho}_{k_i-k_{i+1}})\delta\bar{\rho}_{k_n}$$
$$=-\frac{1}{\omega_\Sigma(q_c)}\int dk_1(\bar{\bar{N}}_1(q_c))_{21}\rho_V^0\sigma_{q-k_1}\sigma_{k_1}+\cdots\ . \tag{C1}$$

When (C1) is substituted in the kinetic equation for $\sigma_q$, we obtain

$$\tau_V\partial_t\sigma_q=\omega_\sigma(q)\sigma_q+\Sigma_{n\geq 1}(-1)^{n-1}\int dk_1\cdots\int dk_n[(\bar{\bar{N}}_n(q_c))_{11}\sigma_{q-k_1}+(\bar{\bar{N}}_n(q_c))_{12}\Sigma_{q-k_1}](\Pi_{i=1}^{n-1}\delta\bar{\rho}_{k_i-k_{i+1}})\delta\bar{\rho}_{k_n}$$
$$=\omega_\sigma(q)\sigma_q+\int dk_1(\bar{\bar{N}}_1(q_c))_{11}\rho_V^0\sigma_{q-k_1}\sigma_{k_1}+\int dk_1[(\bar{\bar{N}}_1(q_c))_{11}\rho_I^0+(\bar{\bar{N}}_1(q_c))_{12}\rho_V^0]\Sigma_{q-k_1}\sigma_{k_1}$$
$$-\int dk_1\int dk_2(\bar{\bar{N}}_2(q_2))_{11}(\rho_V^0)^2\sigma_{q-k_1}\sigma_{k_1-k_2}\sigma_{k_2}\ . \tag{C2}$$

Equation (C2) describes the slow mode dynamics governing the long time evolution of the system. When this reduction of the dynamics, which is of course only valid in the vicinity of the instability, is performed up to the third order in the $\sigma_q$'s, we obtain

$$\tau_V\partial_t\sigma_q=\omega_\sigma(q)\sigma_q+\int dk v(q,k)\sigma_{q-k}\sigma_k+\int dk\int dk' u(q,k,k')\sigma_{q-k}\sigma_{k-k'}\sigma_{k'}\ , \tag{C3}$$

where

$$v(q,k)=(\bar{\bar{N}}_1(\{q_c\}))_{11}\rho_V^0$$

and

$$u(q,k,k')=-(\bar{\bar{N}}_2(\{q_c\}))_{11}(\rho_V^0)^2\left[1+\frac{(\bar{\bar{N}}_1(\{q_c\}))_{21}(\bar{\bar{N}}_1(\{q_c\}))_{12}}{\omega_\Sigma(\bar{\bar{N}}_2(\{q_c\}))_{11}}+\frac{(\bar{\bar{N}}_1(\{q_c\}))_{21}(\bar{\bar{N}}_1(\{q_c\}))_{11}\rho_I^0}{\omega_\Sigma(\bar{\bar{N}}_2(\{q_c\}))_{11}\rho_V^0}\right].$$

This leads, in real space, to

$$\tau_0\partial_t\sigma(\mathbf{r},t)=\left[\frac{b-b_c}{b_c}-\xi_0^2(\nabla^2+q_c^2)^2\right]\sigma(\mathbf{r},t)+v\sigma(\mathbf{r},t)^2-u\sigma(\mathbf{r},t)^3\ . \tag{C4}$$

*Permanent address: Center for Nonlinear Phenomena and Complex Systems, Free University of Brussels, CP 231, B-1050 Brussels, Belgium.

[1]J. H. Evans, Nature **229**, 403 (1971); Radiat. Eff. **10**, 55 (1971).

[2]G. L. Kulcinski, J. L. Brimhall, and H. E. Kissinger, in *Proceedings of the 1971 International Conference on Radiation-Induced Voids in Metals, Albany, NY, June 1971* (USAEC, Washington, DC, 1972), p. 465.

[3]F. W. Wiffen, in *Proceedings of the 1971 International Conference on Radiation Induced Voids in Metals, Albany, NY, June 1971* (Ref. 2), p. 386.

[4]S. Sass and B. L. Eyre, Philos. Mag. **27**, 1447 (1973).

[5]P. B. Johnson, D. J. Mazey, and J. H. Evans, Radiat. Eff. **78**, 147 (1983).

[6]D. J. Mazey and J. H. Evans, J. Nucl. Mater. **138**, 16 (1986).

[7]J. H. Evans and D. J. Mazey, J. Phys. F **15**, L1 (1985); J. Nucl. Mater. **138**, 176 (1986).

[8]A. Jostons and K. Farrel, Radiat. Eff. **15**, 217 (1972).

[9]G. L. Kulcinski and J. L. Brimhall (unpublished).

[10]J. O. Steigler and K. Farrel, Scr. Metall. **8**, 651 (1974).

[11]W. Jager, P. Ehrhart, and W. Schilling, in *Nonlinear Phenomena in Materials Science,* edited by G. Martin and I. P. Kubin (Transtech addr Aedermannsorf, Switzerland, 1988), p. 279.

[12]N. M. Ghoniem and D. Walgraef, Model. Simul. Mater. Sci. Eng. **1**, 569 (1993).

[13]T. Diaz de la Rubia, R. S. Averback, H. Hsieh, and R. Benedek, J. Mater. Res. **4**, 579 (1989).

[14]S. J. Zinkle and B. N. Singh, J. Nucl. Mater. **199**, 173 (1993).

[15]C. H. Woo, A. A. Semenov, and B. N. Singh, J. Nucl. Mater. **206**, 170 (1993).

[16]H. Haken, *Synergetics: An Introduction,* 3rd ed. (Springer, Berlin, 1990).

[17]D. Walgraef, G. Dewel, and P. Borckmans, Adv. Chem. Phys. **49**, 311 (1982).

[18]A. De Wit, G. Dewel, P. Borckmans, and D. Walgraef, Physica D **61**, 289 (1992).

[19]G. L. Kulcinski and J. L. Brimhall (unpublished).

[20]J. O. Stiegler and K. Farrell, Scr. Metall. **8**, 651 (1974).

[21]L. D. Hulett, Jr., T. O. Baldwin, J. C. Crump III, and F. W. Young, Jr., J. Appl. Phys. **39**, 3945 (1968).

[22]J. L. Brimhall, G. L. Kulcinski, H. E. Kissinger, and B. Mastel, Radiat. Eff. **9**, 273 (1971).

[23]J. Wilkes and F. J. P. Clarke, J. Nucl. Mater. **14**, 179 (1964).

[24]A. Jostons and K. Farrell, Radiat. Eff. **15**, 217 (1972).

[25]E. F. Koch and D. Lee, in *Proceedings of the 31st Annual EMSA Meeting* (Clartor's, Baton Rouge, LA, 1973), p. 88.

[26]D. Walgraef and N. M. Ghoniem, Phys. Rev. B **39**, 8867 (1989).

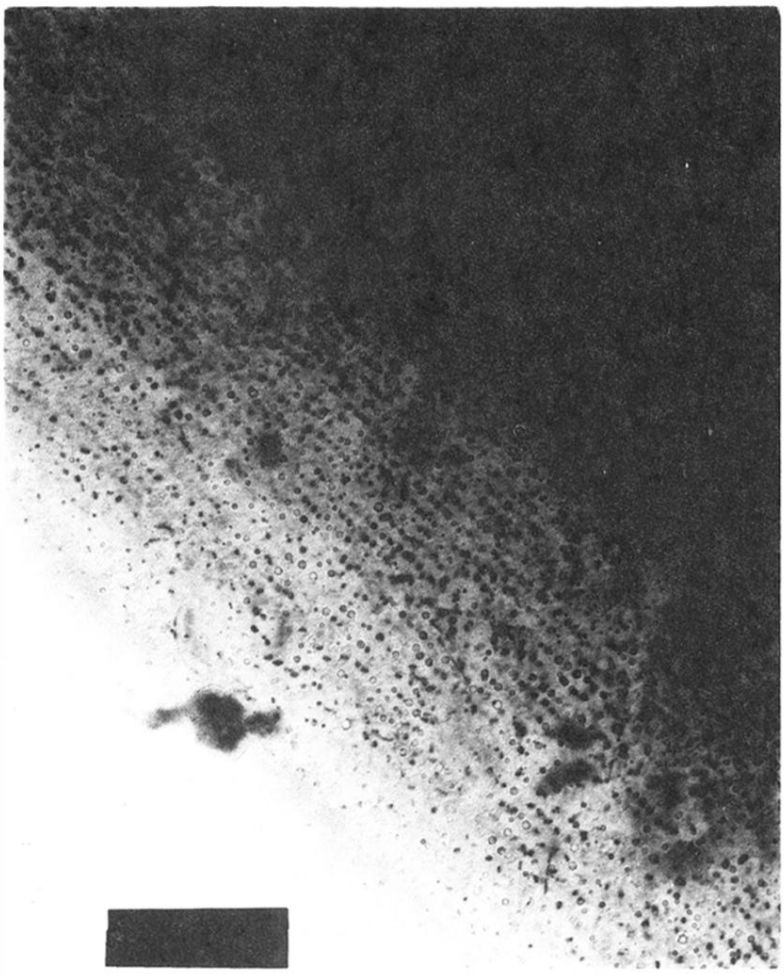

FIG. 1. Void lattice in the alloy TZM, irradiated at 450°C. The fast neutron flux ($E > 0.1$ MeV) is $3.5 \times 10^{2}6$ n/m$^2$, and the magnification is 200 000 (courtesy of J. Evans).

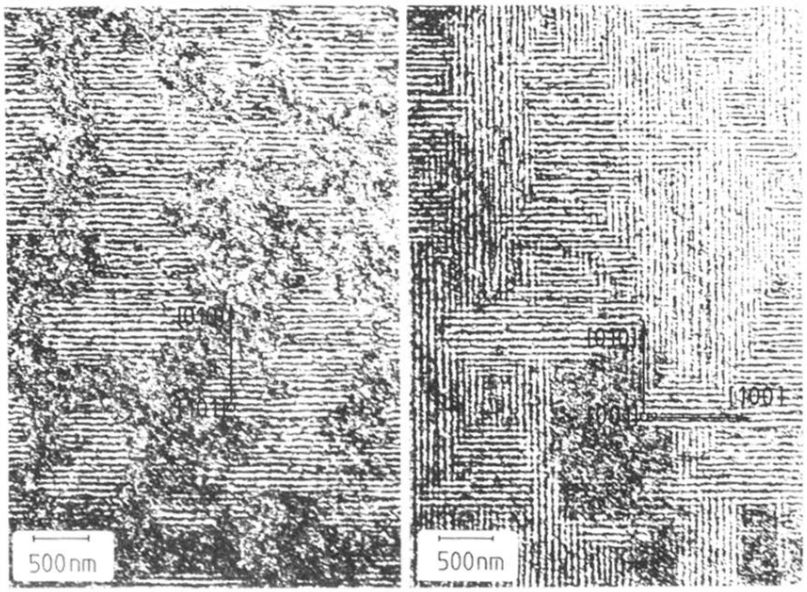


(a) (b)

FIG. 2. Formation of planar periodic defect walls in proton-irradiated copper at a dose of 2 dpa. Imaging is in the {110} projection in (a) and in the {100} projection in (b) (courtesy of W. Jaeger).